

RESEARCH LETTER

Oxidation of the *Mycobacterium tuberculosis* key virulence factor protein tyrosine phosphatase A (MptpA) reduces its phosphatase activity

Anna Niesteruk, Sridhar Sreeramulu, Hendrik R. A. Jonker, Christian Richter and Harald Schwalbe 

Center for Biomolecular Magnetic Resonance (BMRZ), Goethe University Frankfurt am Main, Institute for Organic Chemistry and Chemical Biology, Frankfurt am Main, Germany

Correspondence

H. Schwalbe, Centre for Biomolecular Magnetic Resonance (BMRZ), Goethe University Frankfurt am Main, Institute for Organic Chemistry and Chemical Biology, Max-von-Laue-Straße 7, D-60438 Frankfurt am Main, Germany
 Tel: +49 69 798 29737
 E-mail: schwalbe@nmr.uni-frankfurt.de

(Received 1 March 2022, revised 31 March 2022, accepted 1 April 2022, available online 15 April 2022)

doi:10.1002/1873-3468.14348

Edited by Dietmar Manstein

The *Mycobacterium tuberculosis* tyrosine-specific phosphatase MptpA and its cognate kinase PtkA are prospective targets for anti-tuberculosis drugs as they interact with the host defense response within the macrophages. Although both are structurally well-characterized, the functional mechanism regulating their activity remains poorly understood. Here, we investigate the effect of post-translational oxidation in regulating the function of MptpA. Treatment of MptpA with H₂O₂/NaHCO₃, mimicking cellular oxidative stress conditions, leads to oxidation of the catalytic cysteine (C11) and to a conformational rearrangement of the phosphorylation loop (D-loop) by repositioning the conserved tyrosine 128 (Y128) and generating a temporarily inactive preclosed state of the phosphatase. Thus, the catalytic cysteine in the P-loop acts as a redox switch and regulates the phosphatase activity of MptpA.

Keywords: cysteine-redox regulation; *Mycobacterium tuberculosis*; nuclear magnetic resonance spectroscopy; protein oxidation; protein tyrosine phosphatase; reactive oxygen species

Mycobacterium tuberculosis (*Mtb*) is one of the leading causes of death in humans among bacterial infections [1,2]. Around one-fourth of the world's population carries latent tuberculosis (TB) being a lifelong risk of the outbreak of the disease [3,4]. Unfortunately, the continuous antibiotic-based TB therapy over the past years results nowadays in an increasing amount of highly resistant [multidrug-resistant (MDR) and extensively drug-resistant (XDR)] pathogenic strains [5,6]. The lack of alternative strategies for clinical use to treat and control the progress of TB infection may lead to a very serious problem for global public health.

Targeted treatment of the TB key virulence factors might be a very promising approach in the fight against resistance to *Mtb* [7]. In contrast to traditional antibiotic therapy, which intends to prevent bacterial growth and replication, targeting these virulence factors offers the possibility to directly control bacterial pathogenicity [8,9]. In this context, studies that identify the virulence factors secreted from the pathogen during the infection to interfere with the host defense response are particularly useful, and pharmacological intervention on this cellular level would be very beneficial [10–12]. Yet, this approach is still challenging as the molecular basis for the interplay between the

Abbreviations

CSP, chemical shift perturbation; MptpA, low molecular weight protein tyrosine phosphatase A; *Mtb*, *Mycobacterium tuberculosis*; oxMptpA, oxidized MptpA; oxPTM, oxidative post-translational modification; *p*-NPP, *p*-nitrophenol phosphate; PtkA, protein tyrosine kinase A; PTM, post-translational modification; ROS, reactive oxygen species; TB, tuberculosis; TEV, tobacco etch virus.

pathogen and host is often unclear. Understanding this strategy at the molecular level can provide an important breakthrough in anti-TB drug development.

The tyrosine-specific phosphatase, MptpA, and its cognate kinase, PtkA, are both potential targets for rational drug discovery, as they support the persistency of *Mtb* by interacting with the host defense machinery [14,15]. The subunit B33, a part of the vacuolar protein sorting complexes (HOPS), is the target protein of dephosphorylation by MptpA [16,17]. This step is crucial for the survival of *Mtb* within the host macrophages, as it protects the pathogen from the lysosomal digestion. MptpA itself is a substrate of phosphorylation by PtkA [18]. Moreover, PtkA was shown to be essential for *Mtb* growth within macrophages, underlying a crucial role of MptpA-PtkA operons in *Mtb* pathogenesis [19,20]. Both proteins were subjects of detailed structural characterization in previous studies [21–23]. However, the complex mechanisms which regulate their catalytic activity remain poorly understood [24].

MptpA undergoes a post-translational modification (PTM) by PtkA, which catalyzes the phosphate transfer (phosphorylation) on two vicinal tyrosine residues (Y128 and Y129) located within the D-loop [25]. This modification leads to an increased catalytic activity of MptpA [26], concomitant with an enhanced tyrosine dephosphorylation level in cells. On the molecular level, structural studies of MptpA indicate a conformational rearrangement of the D-loop upon ligand binding [21]. The catalytic cysteine 11 (C11) of MptpA is located in the highly conserved P-loop [(H/V)CX5R(S/T)] within the PTPs family and acts as a nucleophile in the initial cleavage step during dephosphorylation [27]. In addition, the low pKa (4.7–5.4) of this catalytic residue within PTPs, make this protein class highly susceptible to oxidation by reactive oxygen species (ROS) [28–30]. Such secondary messengers including the hydroxyl radical (OH•) and hydrogen peroxide (H₂O₂) are generated during the signaling cascade in the living cells and control signal transduction via protein oxidation, frequently involving catalytic cysteine residues of the PTPs [31–34]. ROS are known to oxidize numerous natural amino acids of which cysteine residue is the most frequent target for this post-translational modification [35]. However, oxidation of other sensitive amino acids has been reported as well [35,36]. Experimental evidence from these previous studies has shown that the oxidation of the catalytic cysteine by low H₂O₂ concentration is reversible, resulting in the formation of disulfide or a five-membered sulfenyl amide ring; both are thiol reducible oxidation products [37,38]. This inactivation

mechanism is used by PTPs for transient masking of the catalytic cysteine. It protects the enzyme against overoxidation during oxidative stress. On the other hand, oxidative post-translational modifications (oxPTMs) occurring at higher ROS concentration can convert cysteine to cysteine sulfinic acid (–SO₂H), which may be further oxidized to cysteine sulfonic acid (–SO₃H) [33,39,40]. For a long time, both cysteine modifications have been considered to irreversibly impair the reactivity of the protein. However, recent studies indicated that the cysteine sulfinic acid in proteins undergoes enzymatic reduction by sulfiredoxin back to the active enzyme [41–43].

In the context of the ability of mycobacteria to overcome the toxic phagosomal environment, the regulation of the activity of MptpA via redox chemistry of the catalytic cysteine seems conceivable. It has been reported that the noncatalytic cysteine 53 (C53) impacts the redox-state of MptpA, as C53 is primarily oxidized by incubation with H₂O₂, resulting in a decreased activity and structural stability of the phosphatase [44,45]. However, so far, there is no specific evidence for transient oxidation of MptpA reported. It has been shown that accessibility and reactivity of the catalytic pocket modulate a key structural motif involving a water molecule and a cysteine-cysteine bridge. Based on these findings a novel regulation mechanism was proposed supporting MptpA to prevail in the oxidative conditions within infected host macrophages [44].

Here, we investigate the oxidative modification of MptpA by H₂O₂ using nuclear magnetic resonance (NMR) spectroscopy. Our data show that the two catalytic important regions: (a) catalytic P-loop and (b) phosphorylation D-loop, are affected by oxidation with H₂O₂/NaHCO₃. By using selectively labeled protein samples, we were able to locate the site and the type of MptpA oxidation, offering detailed insight into the redox regulation mechanism of the catalytic cysteine.

Materials and methods

Protein production and purification

The pET16bTEV vector encoding MptpA (Rv2234, Met1–Ser163) was transformed into *Escherichia coli* BL21 (DE3) pLysS cells for protein expression. The unlabeled protein was expressed using LB growth medium and the uniformly ¹⁵N- or ¹³C, ¹⁵N-labeled protein was expressed in M9 minimal medium using ¹⁵NH₄Cl (1 g·L⁻¹) and ¹³C-glucose (1 g·L⁻¹) as the sole nitrogen and carbon source, respectively. The growth media were supplemented with 1-mM

ampicillin and inoculated at 37 °C with aeration (0.4 g) until an OD₆₀₀ of 0.7 was reached. The protein expression was induced with 1-mM IPTG after 15 min of incubation on ice water. The recombinant MptpA was expressed for over 16 h with aeration (120 r.p.m.) at 16 °C.

For the expression of selectively ¹³C₃, ¹⁵N-cysteine labeled MptpA, the pET16bTEV expression vector was transformed into cysteine auxotroph *E. coli* strain, BL21(DE3) cysE, which was a kind gift from the laboratory of Ch. Dumas (Laboratory of Molecular Biophysics, Bethesda, MD). Single colony was resuspended in a 5-mL LB medium containing unlabeled cysteine (0.05 g·L⁻¹), 2% glucose, and antibiotics (ampicillin 1 mM and kanamycin 0.25 mM), incubated for 12 h at 37 °C with aeration (120 r.p.m.) to produce starter culture. The starter inoculate was transferred in freshly prepared 50-mL M9-aa-medium, containing cysteine (0.05 g·L⁻¹) and antibiotics, and incubated overnight at 37 °C with aeration (120 r.p.m.). The overnight cell culture was washed (2x) with 50-mL wash buffer (PBS-buffer, pH 7.3) and transferred to the 5 liter Erlenmeyer flask containing M9-aa-expression medium (M9-medium supplemented with amino acid stock solution, containing all unlabeled amino acids, except the cysteine; Appendix S1) until an OD₆₀₀ of 0.1 was reached. The cell culture was incubated at 37 °C for 2–3 h to an OD₆₀₀ of 0.3 and the cysteine ¹³C₃, ¹⁵N-isotopically labeled (0.05 g·L⁻¹, Sigma Aldrich, Taufkirchen, Germany) was added to the expression medium. Cell cultures were grown until an OD₆₀₀ of 0.7, incubated for 15 min on ice water, and induced with 1-mM IPTG. The protein was expressed at 16 °C, 16 h with aeration (120 r.p.m.). The expression of tyrosine ¹³C₉, ¹⁵N-selective labeled MptpA was performed in *E. coli* BL21 (DE3) pLysS cells using an M9 expression medium supplemented with amino acid stock solution, containing all amino acids at a concentration of (0.4 g·L⁻¹) and tyrosine residue at (0.2 g·L⁻¹). The required tyrosine ¹³C₉, ¹⁵N-labeled (0.2 g·L⁻¹, Sigma Aldrich, Steinheim, Germany) was supplemented immediately prior to induction, with 1-mM IPTG at 0 °C. For the expression of tyrosine ¹³C₉, ¹⁵N-selective labeled MptpA the same procedure was followed as described above.

The cells were harvested by centrifugation (4000 g, 45 min, 4 °C). The cell pellet was either flash frozen and stored at -80 °C for later use or resuspended in lysis buffer (300-mM NaCl, 50-mM Tris-HCl, pH 8.0, 3-mM Dithiothreitol), supplemented with one EDTA-free complete protease inhibitor (1 tablet/100 mL, Roche, Mannheim, Germany). The cells were disrupted for 15 min using M-110P Microfluidizer (15 000 PSI). The supernatant was separated from cell residues by centrifugation (16 000 g, 40 min, 4 °C). The soluble protein fractions were applied to a 5-mL Ni-NTA His-TrapHP column (GE Healthcare, Uppsala, Sweden), following the manufacturer's recommendations. The His₆-tag was cleaved by the addition of TEV protease (0.001 g·L⁻¹) overnight during the dialysis at 4 °C in dialysis buffer (pH 8.0) and separated on the Ni-NTA column

using elution buffer (pH 8.0). Subsequently, preparative size-exclusion chromatography was performed on a HiLoad 26/60 Superdex 75 column (GE Healthcare) in NMR buffer (pH 7.0) to increase protein purity. The presence of protein was confirmed by SDS/PAGE analysis. The fractions containing pure protein were pooled, flash frozen, and stored at -80 °C or immediately used for further experimental procedures. The buffer compositions are provided in the Materials and Methods, Appendix S1.

Phosphatase activity assay

The phosphatase activity was determined using 1-mM *p*-nitrophenyl phosphate (*p*-NPP) as substrate resolved in assay buffer (25-mM Tris-HCl, pH 8.0). After the addition of DTT-free MptpA (end concentration 1 μM) into the substrate mixture and homogenization of the sample by three times inverting of the cuvette, the absorbance at 410 nm was detected every 60 s, within 600 s time interval using a UV spectrometer (Varian, Cary50Bio). Similar assay lacking MptpA was performed as a control. The average of the absorbance values detected over 600 s obtained for native MptpA was set to 100% activity. The reversibility of the activity of the oxidized MptpA (oxidation by various H₂O₂ concentrations: 1.0, 0.50, 0.10, 0.05, and 0.01 mM, in presence of 25-mM NaHCO₃) was tested, after incubation of the oxidized MptpA (100 μM) with DTT (10 mM) in assay buffer (pH 8.0) for 30 min at 25 °C, using the same detection parameters as reported above.

Oxidation of MptpA

DTT-free MptpA (70 μM) was resolved in 2.5 mL of 25-mM HEPES-NaOH buffer (pH 7.0), containing 150-mM NaCl, mixed with a freshly prepared solution of 50-mM H₂O₂ and 25-mM NaHCO₃ and incubated for 2.5 min at 25 °C on the gel filtration column (PD10 desalting column, GE Healthcare, Freiburg, Germany) or incubated with 50 u catalase (Sigma Aldrich, Hamburg, Germany). The protein eluate from the PD10 desalting column was collected, concentrated (100 to 200 μM), and analyzed.

NMR spectroscopy

The NMR experiments were performed at 298 K on Bruker spectrometers (600, 800, or 950 MHz) equipped with TCI-HCN cryogenic probes. The spectrometers were locked on D₂O. The protein samples (0.1–0.2 mM) were measured in NMR buffer (25-mM HEPES/NaOH, pH 7.0, 150-mM NaCl, 5% D₂O/95% H₂O) using 3-mm NMR tubes. The acquisition and processing of the NMR data were carried out with TopSpin version 3.2 (Bruker Biospin) and analyzed using Sparky version 3.114. The backbone assignment of MptpA as deposited in the BMRB, with the entry

number 18533 was used for spectra analysis. ^{15}N relaxation experiments were performed at 298 K on a 800-MHz spectrometer. The R_1 longitudinal ^{15}N relaxation rates were obtained from a series of experiments acquired with varying delays of 10, 100, 400, 600, 800, 1000, 1200, and 1500 ms. R_2 transverse ^{15}N relaxation rates were determined from a series of spectra using the following delays: 33.92, 67.84, 101.76, 135.68, 169.6, 203.52, 237.44, and 271.36 ms. Temperature coefficient (in ppb/K) was obtained from a series of 2D- $(^1\text{H}, ^{15}\text{N})$ -HSQC spectra recorded at 5 K intervals ranging from 283 to 303 K on a 800-MHz spectrometer.

Results

Phosphatase activity of MptpA

The phosphatase activity of MptpA was previously assayed using *p*-nitrophenol phosphate (*p*-NPP) as substrate [21]. The same assay was used here to examine the catalytic activity of MptpA after oxidation by $\text{H}_2\text{O}_2/\text{NaHCO}_3$. The absorption detected at 410 nm refers to the reduced amount of the chromogenic dephosphorylation product (*p*-nitrophenolate, *p*-NP). The decrease of this signal observed for the oxidized MptpA (oxMptpA) indicates the reduction in the MptpA activity after oxidation (Fig. S1). To delineate whether the oxidative modification of MptpA by $\text{H}_2\text{O}_2/\text{NaHCO}_3$ is reversible, the oxMptpA was incubated with dithiothreitol (DTT, 10 mM) at 25 °C for 30 min (Fig. S1). An increase of the absorption (at 410 nm) indicates partial recovery of the enzymatic activity of oxMptpA in a time- and DTT-concentration-dependent manner. The restored phosphatase activity of the oxMptpA was estimated to be 2–10% (depending on the concentration of H_2O_2 used for oxidation), suggesting at least partial oxidation reversibility by cellular glutathione.

NMR studies of the oxidized MptpA (oxMptpA)

The hydrogen peroxide (H_2O_2)-induced oxidative modification of MptpA was studied in more detail using NMR spectroscopy. In general, protein oxidation requires DTT-free buffer conditions. Since the sequence of MptpA contains three cysteine (C11, C16, and C53), removal of DTT from the NMR buffer may potentially lead to the disulfide bond formation in native phosphatase. To verify this, 2D- $(^1\text{H}, ^{15}\text{N})$ -HSQC spectra of MptpA were measured in the absence and in the presence of DTT (Fig. S2). Both spectra remain essentially the same, which indicates that the removal of DTT from the buffer solution has no effect on MptpA native folding.

Optimization of the oxidation reaction

MptpA was oxidized with a supra-physiological concentration of H_2O_2 . To enhance the oxidative inactivation reaction 25-mM bicarbonate (NaHCO_3) was used [46]. Oxidation of MptpA in presence of 200-mM H_2O_2 and 25-mM NaHCO_3 results in a strong reduction of the protein stability causing protein precipitation. Moreover, the 2D- $(^1\text{H}, ^{15}\text{N})$ -HSQC spectrum of the oxMptpA indicates protein unfolding, manifested by loss of signal dispersion of ~ 1 ppm in the ^1H dimension (Fig. 1A). Since the generation and decomposition of ROS *in vivo* are under strict enzymatic control [47], the exposure of MptpA to the oxidant in this experiment may actually have been too harsh. With the introduction of an additional preparative step during the oxidation reaction such as (a) gel filtration or (b) enzyme (catalase) and lowering the H_2O_2 concentration to 50 mM, we could stabilize and isolate an oxidized folded state of MptpA (Fig. 1A). Regardless of the method used for the removal of the oxidant, a folded oxidized state of MptpA was generated (Fig. S3). The amide cross-peaks remain the same for most of the residues. However, treatment with catalase yields a more heterogeneous sample with additional cross-peaks and signal splitting. For further oxidation studies by NMR, we choose the PD10 treatment, which results in a more homogeneous sample.

The effect of the oxidation on MptpA

In general, all amino acids within the protein can be oxidized by ROS [48]. Yet, sulfur-containing amino acids or aromatic residues show a higher susceptibility to oxidation [49,50]. Furthermore, oxidative modification can modulate the local hydrogen-bond environment and electrostatic polarities, thereby inducing structural and/or dynamic alterations of the protein and impairing the catalytic activity of the enzyme. To investigate whether such changes are also potentially present in MptpA, we examined the effect of oxidation on the NMR backbone amide signals. The backbone amides are highly sensitive to the changing surrounding environment and therefore an important source of structural information. As expected, alterations of the amide cross-peaks located near the catalytic pocket are observed (Fig. 1B). Around 8% (12 from 145) of the signals disappear after oxidation of MptpA by $\text{H}_2\text{O}_2/\text{NaHCO}_3$. In addition, the amides of the residues in the spatial proximity of those missing signals show chemical shift perturbations (CSPs) of ≥ 0.3 ppm (Fig. 1B–D). All those changes remain restricted to residues of the three catalytic important loops: P-, D-,

W-loop and to residues located between two α -helices (α -helix $\alpha 2$ and α -helix $\alpha 3$) or in the α -helix $\alpha 4$ (Fig. 1D).

Effect of the oxidation on MptpA hydrogen bonding

To assess possible changes in the intramolecular hydrogen bonding of MptpA, before and after oxidation by H_2O_2 - NaHCO_3 , we determined the temperature dependency of the backbone amide proton chemical shift values. The temperature coefficient (Tcoeff. in ppb/K, Fig. 1D) was obtained from a series of 2D- $(^1\text{H}, ^{15}\text{N})$ -HSQC spectra measured at different temperatures (from 303 K to 283 K with 5° increments). Following the trend of the temperature coefficient (typical for indicating hydrogen-bonded amide protons when larger than -4.5 ppb/K [51]), we conclude that the intramolecular hydrogen bonding of the oxMptpA resembles the native protein. However, substantial differences in the temperature coefficient are observed within the W-loop, which suggests that amides of amino acids N47, G51, D55, and E56 lose the hydrogen bonds after oxidation by H_2O_2 - NaHCO_3 . The W-loop is located in close proximity to the catalytic P-loop and contains one of the three conserved cysteine residues, the noncatalytic cysteine C53. To study whether the observed differences also involve changes in the dynamic behavior of MptpA before and after oxidation by H_2O_2 - NaHCO_3 we used conventional heteronuclear ^{15}N relaxation experiments. The obtained relaxation rates of ^{15}N - T_1 and ^{15}N - T_2 relaxation times of the native and oxidized MptpA are similar (Fig. S4), suggesting that the oxidation of MptpA by H_2O_2 - NaHCO_3 has no effect on the local backbone dynamic of MptpA. The oxidative modification by ROS occurs in particular on the most reactive functional group within the side chain of the target residue, affecting only indirectly the properties of the backbone amide. Therefore, additional NMR experiments on the side chain could provide more detailed information on the site and type of oxidation.

The catalytic site of MptpA

The side chain $^{13}\text{C}\beta$ chemical shifts can be used as reporters to define the product of the oxidation of MptpA by H_2O_2 - NaHCO_3 . Analysis of the 2D- $(^1\text{H}, ^{13}\text{C})$ -HSQC spectrum of oxMptpA allows us to distinguish between (a) directly and (b) indirectly involved residues in the oxidation. The significant signal perturbations observed for cysteines (C11, C16) and tyrosine (Y128) residues, suggest that both, the

catalytic (P-loop) as well as the phosphorylation site (D-loop) of MptpA are potential targets of oxidation by H_2O_2 - NaHCO_3 . The P-loop, the catalytic site of MptpA contains two (C11, C16) of the three (C11, C16, C53) conserved cysteines in the sequence (Fig. 2A). The sulfur-containing side chains of all three cysteines within the MptpA can be potentially oxidized by H_2O_2 - NaHCO_3 . Yet, both the *p*-NPP activity assay as well as the backbone NMR studies performed on oxMptpA strongly indicate the oxidative modification of the catalytic cysteine, C11, manifested by the decrease of the phosphatase activity of oxMptpA and its amide cross-peak attenuation after oxidation. We produced cysteine ($^{15}\text{N}, ^{13}\text{C}_3$)-selectively labeled MptpA (*cys*MptpA) using auxotrophic *E. coli* cells, to study the effect of the oxidation of MptpA on cysteine residues in specific detail. The 2D- $(^1\text{H}, ^{13}\text{C})$ -HSQC spectrum of the *cys*MptpA resolves as expected three $\text{CH}\alpha$ (Fig. 2B) and six $\text{CH}\beta 1$, $\text{CH}\beta 2$ (Fig. 2C) signals with the chemical shift as those observed for the uniformly double ($^{15}\text{N}, ^{13}\text{C}$) labeled MptpA (Fig. 2C). After oxidation of *cys*MptpA by H_2O_2 - NaHCO_3 (*cys*MptpA^{OX}), both $\text{CH}\beta 1$ and $\text{CH}\beta 2$ as well as the $\text{CH}\alpha$ cross-peaks of C11 disappear, suggesting complete oxidation of the catalytic cysteine (Fig. 2B, C). Furthermore, a set of new signals appearing in the spectrum of *cys*MptpA^{OX}, in the spectral region between $\delta^1\text{H}$ 2.8–2.2 ppm and $\delta^{13}\text{C}$ 63.5–64.5 ppm, indicate the oxidation products of C11 (Fig. 2C, right). The same cross-peaks were also observed in the 2D- $(^1\text{H}, ^{13}\text{C})$ -HSQC spectrum of the uniformly double ($^{15}\text{N}, ^{13}\text{C}$) labeled MptpA after oxidation by H_2O_2 - NaHCO_3 (Fig. 2C, left) and could now be specifically assigned to originate from C11. Typically, the chemical shift change of the $\text{C}\beta$ resonance from ~ 20 ppm to ~ 60 ppm indicates *oxo*-forms of cysteine such as sulfenic (Cys-SO₂H) or sulfonic (Cys-SO₃H) acid [52]. Furthermore, we can exclude oxidation of the noncatalytic C53 as both $^{13}\text{C}\alpha$ and $^{13}\text{C}\beta$ resonances remain the same chemical shift after oxidation. In addition, the chemical shift perturbation observed for cysteine C16 is likely induced by the oxidation of the nearby catalytic cysteine C11 in the P-loop.

The phosphorylation site of MptpA

The active site motif of MptpA is flanked by two dynamic loops, the D-loop and the W-loop. The D-loop contains three essential residues: the catalytic aspartic acid (D126) and two tyrosine residues (Y128 and Y129). Both tyrosine residues are phosphorylation targets of the complementary tyrosine-specific kinase, PtkA, that regulates the phosphatase activity of

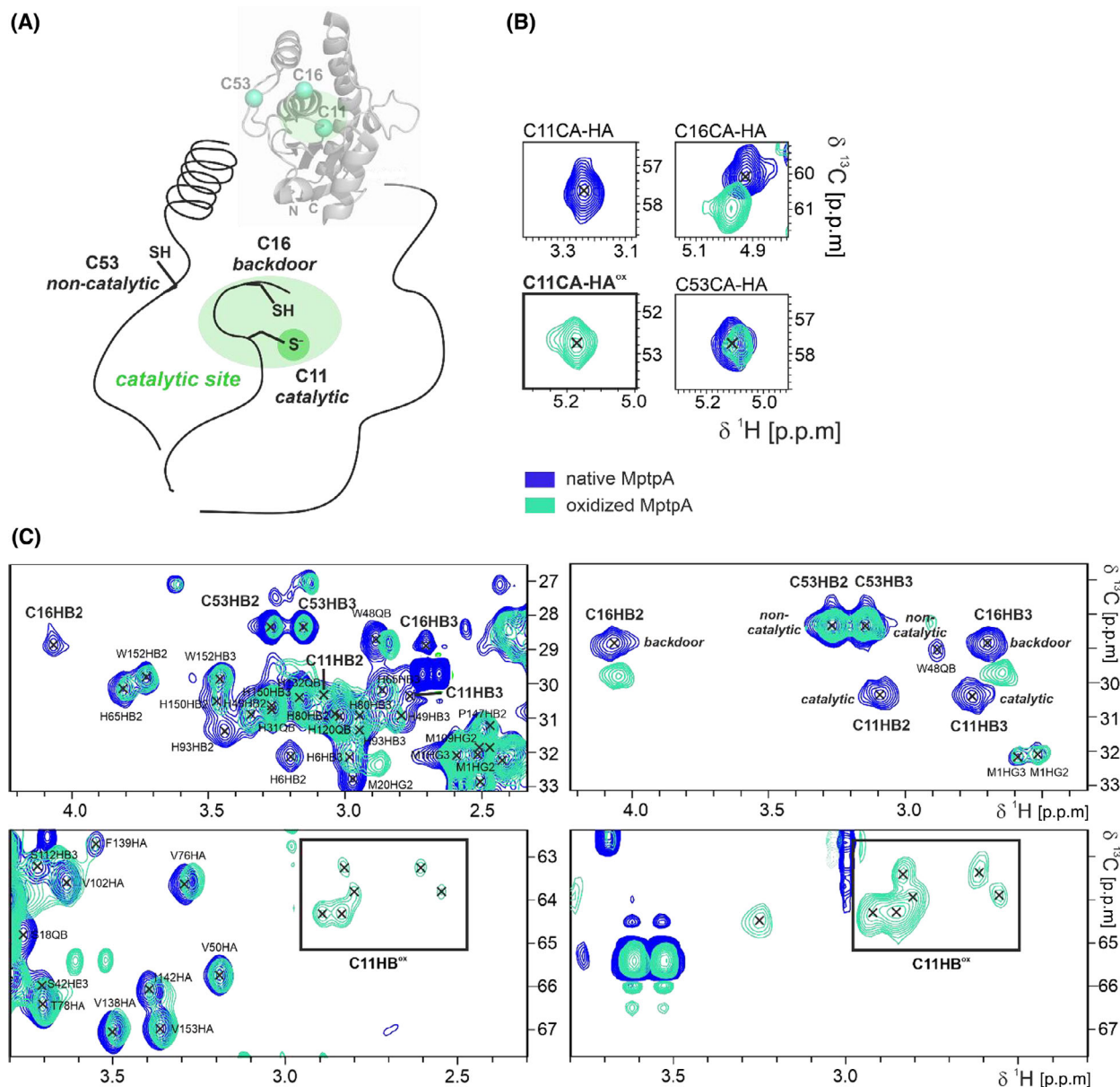


Fig. 2. Effect of oxidation on MtpA catalytic site. (A) Schematic representation of the catalytic site of MtpA; the loop position of the three conserved cysteine residues C11 (catalytic), C16 (backdoor), and C53 (noncatalytic) is highlighted. (B) Zoom in of the overlay of ¹³CH_α cross-peaks from 2D-(¹H, ¹³C)-HSQC spectra of cysteine (¹⁵N, ¹³C₃) selectively labeled MtpA (cysMtpA) before (blue) and after (green) oxidation with 50-mM H₂O₂, 25-mM NaHCO₃, and gel filtration. (C) Overlay of ¹³CH_α from 2D-(¹H, ¹³C)-HSQC spectra of the double (¹⁵N, ¹³C) labeled MtpA (left) and cysMtpA (right) before and after oxidation with H₂O₂-NaHCO₃. Cross-peaks of cysteine residues are assigned. A set of the new signals observed after oxidation are highlighted with box.

MtpA [26]. Furthermore, structural studies of MtpA indicate a conformational rearrangement of the D-loop from an open to a close state upon ligand binding. Our NMR studies here show that the conserved tyrosine residues of MtpA are affected by the oxidation of H₂O₂-NaHCO₃. Similar as for the MtpA cysteine studies, we produced tyrosine (¹⁵N, ¹³C₉)

selectively labeled MtpA (*tyr*MtpA) to investigate the effect of the oxidation on the phosphorylation site of MtpA. The 2D-(¹H, ¹³C)-HSQC spectrum of the *tyr*MtpA resolves as expected six CHβ1, CHβ2, and three CH_α cross-peak signals, originating from the three tyrosine residues (Y67, Y128, and Y129). After oxidation of *tyr*MtpA by H₂O₂-NaHCO₃ only the

CH β 1 and CH β 2 signals of Y128 are strongly perturbed, where the resonances of Y67 and Y129 remain practically unaffected (Fig. 3). Furthermore, the aromatic 2D-(^1H , ^{13}C)-HSQC spectrum of *tyr*MtpA^{OX} clearly resolves the perturbed signal at $\delta^1\text{H}$ 6.7/ $\delta^{13}\text{C}$ 28.1 ppm after oxidation, for the CH ϵ 1 and CH ϵ 2 cross-peak of Y128 (Fig. 3, C). The observed chemical shift perturbations evidently indicate that tyrosine Y128 is affected upon oxidation of C11 and thereby suggests conformational and/or environmental changes of the D-loop.

Discussion

Cysteine-redox regulation is meanwhile well-characterized for many PTPs, with the diversity of the biologically relevant *oxo*-cysteine products [57]. The formation of *oxo*-cysteine products is determined by the cellular concentration of ROS and relying on this leads to temporal or permanent inactivation of the protein. *Mtb* protein tyrosine phosphatase A, MtpA is the key virulence factor of mycobacterial pathogenicity and therefore a promising target for pharmacological intervention [16]. MtpA is structural well described [21], however, our lack in understanding the underlying mechanism that regulates the catalytic activity, challenges the design of potential anti-tubercular agents. In particular, there are two frequent post-translational modifications (PTMs) of the protein tyrosine phosphatase (PTPs) family, regulating their activity, namely (a) protein phosphorylation [53,54] and (b) protein oxidation [55]. Both modifications are known to potentially regulate the catalytic activity of MtpA, though their exact mode of operation is poorly understood. Phosphorylation of MtpA by its complementary kinase, PtkA, involves two tyrosine residues, Y128 and Y129, located in the flexible D-loop, surrounds the catalytic pocket. The activity of MtpA increases in the tyrosine-phosphorylated state [26]. Post-translational oxidation of PTPs is an alternative regulatory mechanism, mostly directed towards the oxidation of the catalytic cysteine. In the context of the mycobacterial capability to overcome the toxic phagosome environment [13,56], the post-translational modification of the catalytic C11 would be a plausible regulatory mechanism. Although all-natural amino acids are potential targets of post-translational oxidation by ROS, the significant differences in the reactivity between them dictate the preferred sites for oxidative modification. For instance, the catalytic cysteine conserved within the catalytic P-loop [(H/V)CX5R(S/T)] of PTPs is highly reactive (pKa of 4.7–5.4) and acts as a nucleophile in the initial cleavage

step during the dephosphorylation reaction [55]. Moreover, its low pKa value makes this cysteine highly susceptible to oxidation by ROS.

In our studies, we characterize the effect of ROS-oxidation (H_2O_2 - NaHCO_3) on the structural and dynamic properties of MtpA using NMR spectroscopy. Chemical shifts of the amide groups of the three catalytic important loop regions (P-, D-, and W-loop) of MtpA, change after oxidation. Residues located in the spatial surrounding those functional loops show the most substantial chemical shift perturbations (CSPs). NMR intramolecular hydrogen bonding and protein dynamic studies performed after oxidation of MtpA by H_2O_2 - NaHCO_3 resume similar propensities as those of the native protein, apart from the W-loop region, indicating there an increase in the flexibility after oxidation. Although it is not surprising that the residues of the solvent-exposed flexible loops are more sensitive to the changing environment, strong CSPs and signal attenuation observed for the residues of the regulatory region, suggest oxidative modification of one of the catalytic important residues. Evidently, oxidation of amino acids may slightly impair local intramolecular hydrogen bonding leading to changes in the amide chemical shift and/or amide hydrogen-solvent exchange rate of the neighbored residues. Utilizing the traditional 2D-(^1H , ^{13}C)-HSQC experiments acquired for oxidized doubly (^{15}N , ^{13}C) labeled MtpA we show that the two regulatory regions of MtpA, (a) P-loop and (b) D-loop, are the affected regions after oxidation by H_2O_2 - NaHCO_3 . Especially, the cysteines of the catalytic P-loop, C11 and C16 and the tyrosines of the phosphorylation site, Y128 and Y129 are impacted by oxidation. This finding is interesting since these amino acids are important regulatory residues of MtpA and prone to oxidation by ROS. Using amino acid selective (a) cysteine (^{15}N , $^{13}\text{C}_3$ -cys) and (b) tyrosine (^{15}N , $^{13}\text{C}_9$ -tyr) labeled MtpA, we were able to determine the site and the type of MtpA oxidation by H_2O_2 - NaHCO_3 . The highly nucleophilic cysteine, C11, is the target of the post-translational modification by H_2O_2 - NaHCO_3 . Oxidation of C11 is manifested by the disappearance of the corresponding $^{13}\text{C}\alpha$ and $^{13}\text{C}\beta$ cross-peaks from the 2D-(^1H , ^{13}C)-HSQC spectrum, consistently observed for the uniformly double (^{15}N , ^{13}C) and cysteine (^{15}N , $^{13}\text{C}_3$)-selective labeled protein. Furthermore, the appearance of new resonances in the low-field region around $\delta^1\text{H}$ 2.8–2.2/ $\delta^{13}\text{C}$ 63.5–64.5 ppm in both spectra (hence those signals are absent in the spectrum of the tyrosine selective labeled protein) indicates strongly, oxidative modification of the catalytic cysteine C11. Our detected $^{13}\text{C}\text{CC}\beta$ chemical shift changes from ~ 20 ppm

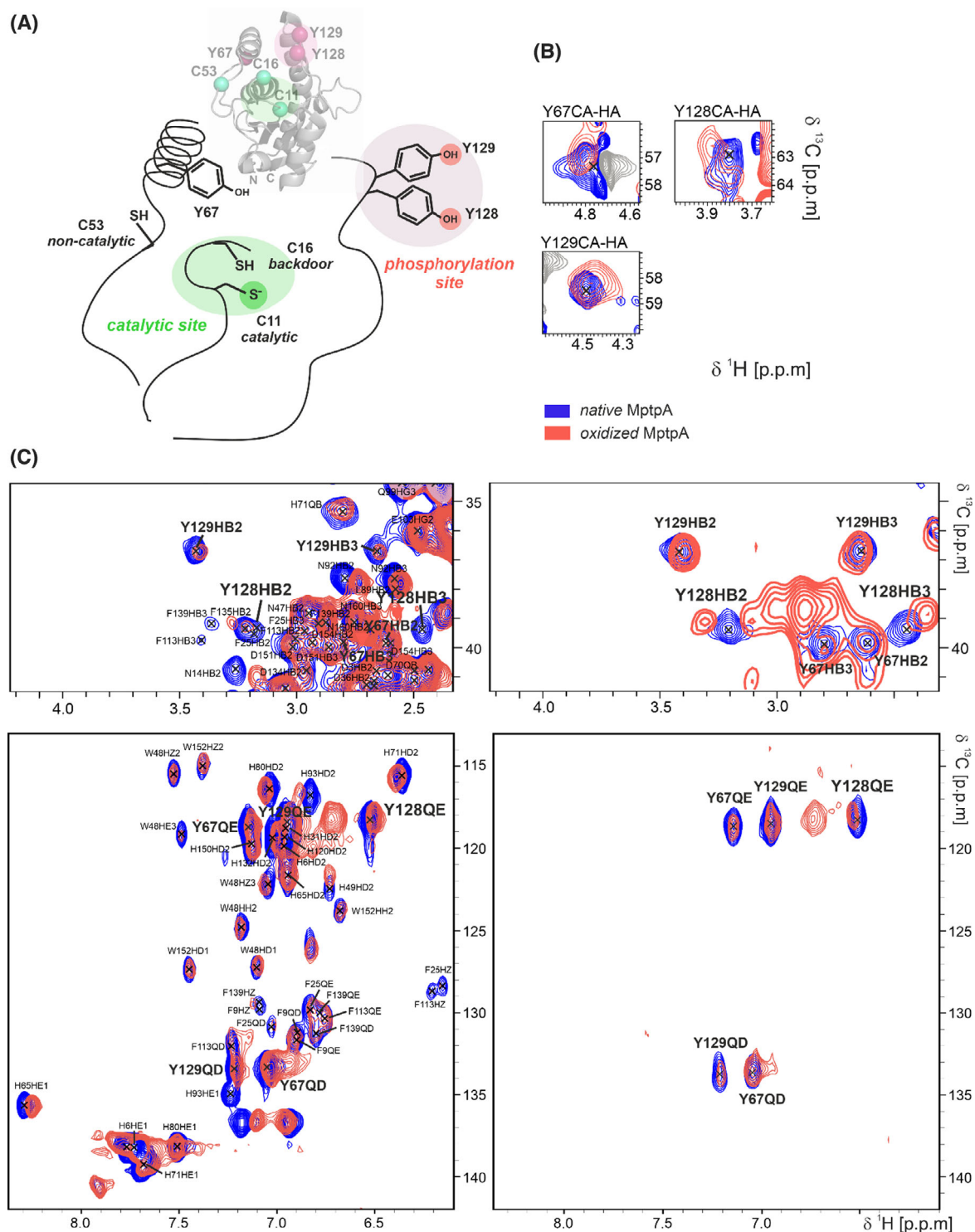


Fig. 3. Effect of oxidation on MptpA catalytic site. (A) Schematic representation of the catalytic and phosphorylation site of MptpA, showing essential cysteine (C11, C16, C53) and tyrosine (Y67, Y128 and Y129) residues. (B) Zoom in of the overlay of $^{13}\text{C}\alpha$ cross-peaks from 2D- $(^1\text{H}, ^{13}\text{C})$ -HSQC spectra of tyrosine($^{15}\text{N}, ^{13}\text{C}$) selectively labeled MptpA (*tyrMptpA*) before (blue) and after (red) oxidation with 50-mM H_2O_2 , 25-mM NaHCO_3 , and gel filtration. (C) Overlay of $^{13}\text{C}\beta$ cross-peaks (top) from 2D- $(^1\text{H}, ^{13}\text{C})$ -HSQC of the double ($^{15}\text{N}, ^{13}\text{C}$) labeled MptpA (left) and *tyrMptpA* (right) before and after oxidation. Overlay of the aromatic 2D- $(^1\text{H}, ^{13}\text{C})$ -HSQC spectra (bottom) of the double ($^{15}\text{N}, ^{13}\text{C}$) labeled MptpA and *tyrMptpA* before and after oxidation.

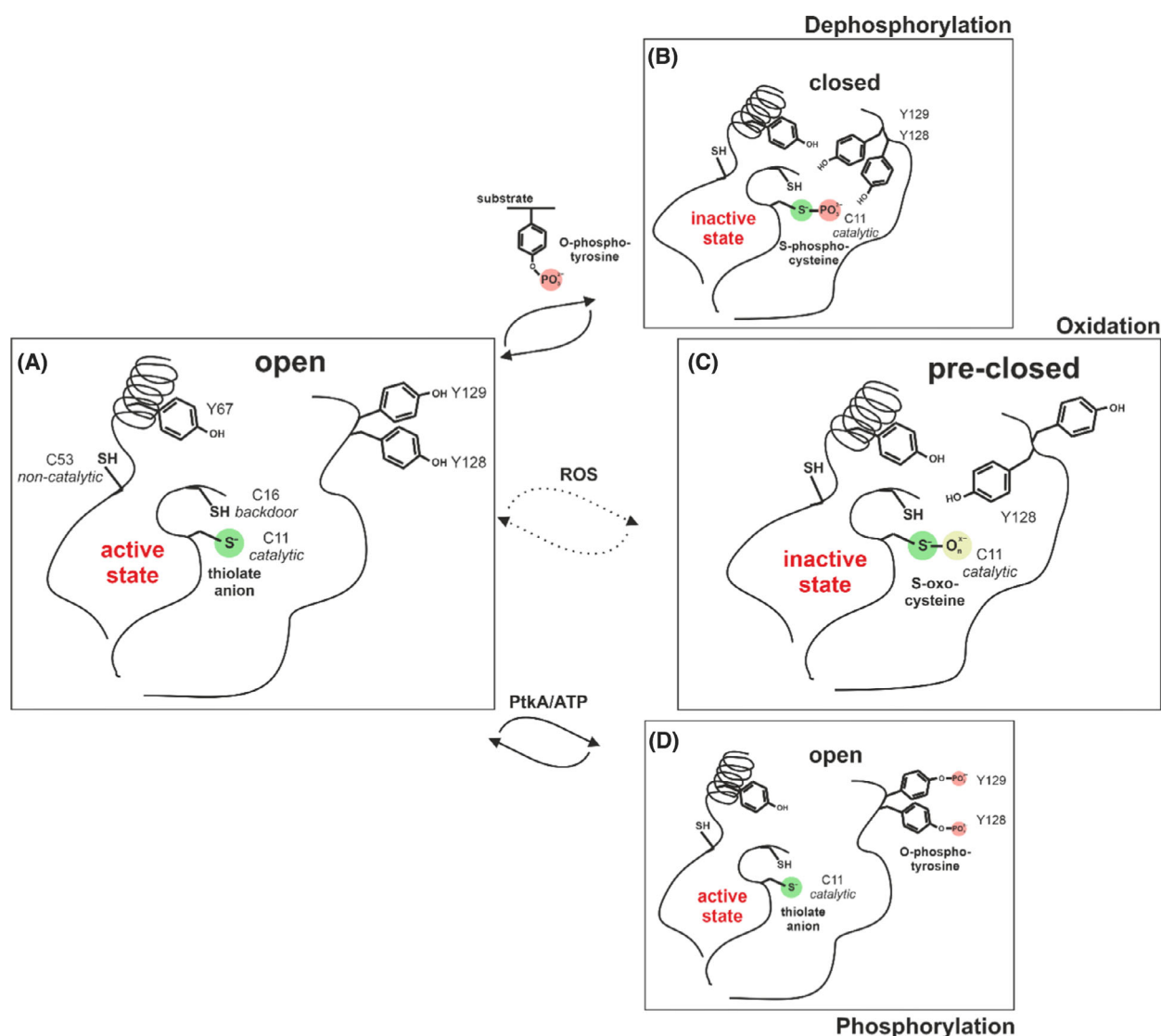


Fig. 4. Regulation of MtpA phosphatase activity. (A) Semantical representation of MtpA regulatory motifs. (B) Tyrosine specific dephosphorylation of the substrate protein catalyzed by MtpA. The nucleophilic cysteine forms a thiophosphate intermediate during the first step of the dephosphorylation reaction, inducing D-loop rearrangement from open to close state, temporary inactivating activity of MtpA. (C) Oxidation of MtpA by ROS leads to formation of S-oxo-cysteine products, inducing formation of a temporary preclosed by repositioning the conserved tyrosine 128 (Y128). (D) Phosphorylation of MtpA on vicinal located tyrosine residues (Y128, Y129) catalyzed by PtkA may support open (active) conformation, thereby increasing the accessibility of the catalytic cysteine for the catalysis of the dephosphorylation reaction of the substrate.

to ~60 ppm are in line with values observed for *oxo*-forms of cysteine as sulfenic (Cys-SO₂H) or sulfonic (Cys-SO₃H) acid. Note that while both cysteine modifications were for a long time considered to irreversibly inactivate the protein, recent proteomic studies have demonstrated that a significant number of proteins exhibit reversible enzymatically reducible cysteine sulfenic acids (Cys-SO₂H) modification [43].

Using NMR spectroscopy, we further show that the oxidation of MtpA by ROS exclusively modifies

catalytic cysteine C11, thereby reducing the activity of the phosphatase. In a similar fashion, the formation of a thiophosphate intermediate during the dephosphorylation of the substrate also results in decreased activity of MtpA (Fig. 4, top). The reduction of the phosphatase activity detected after oxidation of MtpA by H₂O₂-NaHCO₃, strongly suggests that the cysteine sulfur oxidation also promotes conformational rearrangement of the D-loop from an active (open) to an inactive (close) state. However, since our NMR studies

on the oxidized tyrosine (^{15}N , $^{13}\text{C}_9$)-selectively labeled MtpA reveals exclusive involvement of the Y128, we propose that the close state generated during the oxidation may differ from those generated during the substrate binding and termed them preclosed (inactive) state (Fig. 4, middle). Following this, the phosphorylation of MtpA on vicinal located tyrosine residues (Y128, Y129) catalyzed by PtkA may support open (active) conformation, thereby increasing the accessibility of the catalytic cysteine for the catalysis of the dephosphorylation reaction of the substrate (Fig. 4, bottom). However, the phosphorylation state of MtpA during the post-translational oxidation *in vivo* remains unknown. In this context, oxidation studies with MtpA in a tyrosine-phosphorylated states would be particularly interesting. We attempted such studies, but in our hands, phosphorylated MtpA could not be isolated, as it is not clear whether MtpA possesses auto-dephosphorylation activity.

In conclusion, our studies provide important insights into the redox regulation of MtpA and reveal the key elements involved in oxidation, thereby contributing to a general understanding of the function of the phosphatase.

Acknowledgements

We thank Dr. Tanja Stehle for her participation in the early stages of this work. This work was supported in part by the DKTK (German Consortium for Translational Cancer Research), FOR2509 (German Research Foundation, DFG), and iNEXT-Discovery, project number 871037, funded by the Horizon 2020 program of the European Commission. The work at BMRZ was supported by the State of Hesse.

Author contributions

HS conceived and supervised the study; AN wrote the manuscript, performed experiments, and analyzed the data; SS and HJ supported the design of experiments and data analysis; CR performed experiments; HS, SS, and HJ made manuscript revisions.

Data accessibility

The data that support the findings of this study are available in Figs 1–3 and the supplementary material of this article (Table S1 and Figs S1–S4). Additional data are available from the corresponding author [schwalbe@nmr.uni-frankfurt.de] upon reasonable request.

References

- World Health Organization. Tuberculosis: key facts. Geneva: World Health Organisation; 2020.
- World Health Organization. The Top 10 causes of death. Geneva: World Health Organisation; 2018. p. 1–7.
- Behr MA, Edelstein PH, Ramakrishnan L. Revisiting the timetable of tuberculosis. *BMJ*. 2018;**362**:k2738. <https://doi.org/10.1136/bmj.k2738>
- Cohen A, Mathiasen VD, Schön T, Wejse C. The global prevalence of latent tuberculosis: a systematic review and meta-analysis. *Eur Respir J*. 2019;**54**:1900655. <https://doi.org/10.1183/13993003.00655-2019>
- World Health Organization. Tuberculosis: multidrug-resistant tuberculosis (MDR-TB). Geneva: World Health Organisation; 2018.
- Pai M, Behr MA, Dowdy D, Dheda K, Divangahi M, Boehme CC, et al. Tuberculosis. *Nat Rev Dis Prim*. 2016;**2**:16076. <https://doi.org/10.1038/nrdp.2016.76>
- Barczak AK, Hung DT. Productive steps toward an antimicrobial targeting virulence. *Curr Opin Microbiol*. 2009;**12**:490–6. <https://doi.org/10.1016/j.mib.2009.06.012>
- Dickey SW, Cheung GYC, Otto M. Different drugs for bad bugs: antivirulence strategies in the age of antibiotic resistance. *Nat Rev Drug Discov*. 2017;**16**:457–71. <https://doi.org/10.1038/nrd.2017.23>
- Allen RC, Popat R, Diggle SP, Brown SP. Targeting virulence: can we make evolution-proof drugs? *Nat Rev Microbiol*. 2014;**12**:300–8. <https://doi.org/10.1038/nrmicro3232>
- Sharma AK, Dhasmana N, Dubey N, Kumar N, Gangwal A, Gupta M, et al. Bacterial virulence factors: secreted for survival. *Indian J Microbiol*. 2017;**57**:1–10. <https://doi.org/10.1007/s12088-016-0625-1>
- Tomioka H. New approaches to tuberculosis—novel drugs based on drug targets related to toll-like receptors in macrophages. *Curr Pharm Des*. 2014;**20**:4404–17. <https://doi.org/10.2174/1381612819666131118163331>
- Kim D.-H, Kang S.-M, Lee B.-J. Solution NMR studies of mycobacterium tuberculosis proteins for antibiotic target discovery. *Molecules*. 2017;**22**(9):1447. <https://doi.org/10.3390/molecules22091447>
- Queval CJ, Brosch R, Simeone R. The macrophage: a disputed fortress in the battle against mycobacterium tuberculosis. *Front Microbiol*. 2017;**8**:2284.
- Rankine-Wilson LI, Shapira T, Sao Emani C, Av-Gay Y. From infection niche to therapeutic target: the intracellular lifestyle of Mycobacterium tuberculosis. *Microbiology*, 2021;**167**(4):1041. <https://doi.org/10.1099/mic.0.001041>
- Wong D, Chao JD, Av-Gay Y. Mycobacterium tuberculosis-secreted phosphatases: from pathogenesis to targets for TB drug development. *Trends Microbiol*. 2013;**21**:100–9. <https://doi.org/10.1016/j.tim.2012.09.002>

- 16 Bach H, Papavinasundaram KG, Wong D, Hmama Z, Av-Gay Y. Mycobacterium tuberculosis virulence is mediated by PtpA dephosphorylation of human vacuolar protein sorting 33B. *Cell Host Microbe*. 2008;**3**:316–22. <https://doi.org/10.1016/j.chom.2008.03.008>
- 17 Wong D, Bach H, Sun J, Hmama Z, Av-Gay Y. Mycobacterium tuberculosis protein tyrosine phosphatase (PtpA) excludes host vacuolar-H⁺-ATPase to inhibit phagosome acidification. *Proc Natl Acad Sci*. 2011;**108**:19371–6. <https://doi.org/10.1073/pnas.1109201108>
- 18 Bach H, Wong D, Av-Gay Y. Mycobacterium tuberculosis PtkA is a novel protein tyrosine kinase whose substrate is PtpA. *Biochem J*. 2009;**420**:155–62. <https://doi.org/10.1042/bj20090478>
- 19 Wong D, Li W, Chao JD, Zhou P, Narula G, Tsui C, et al. Protein tyrosine kinase, PtkA, is required for Mycobacterium tuberculosis growth in macrophages. *Sci Rep*. 2018;**8**:155. <https://doi.org/10.1038/s41598-017-18547-9>
- 20 Chao JD, Wong D, Av-Gay Y. Microbial protein-tyrosine kinases. *J Biol Chem*. 2014;**289**:9463–72. <https://doi.org/10.1074/jbc.R113.520015>
- 21 Stehle T, Sreeramulu S, Löhr F, Richter C, Saxena K, Jonker HRA, et al. The Apo-structure of the low molecular weight protein-tyrosine phosphatase A (MptpA) from mycobacterium tuberculosis allows for better target-specific drug development. *J Biol Chem*. 2012;**287**:34569–82. <https://doi.org/10.1074/jbc.M112.399261>
- 22 Niesteruk A, Jonker HRA, Richter C, Linhard V, Sreeramulu S, Schwalbe H. The domain architecture of PtkA, the first tyrosine kinase from Mycobacterium tuberculosis, differs from the conventional kinase architecture. *J Biol Chem*. 2018;**293**:11823–36. <https://doi.org/10.1074/jbc.RA117.000120>
- 23 Niesteruk A, Hutchison M, Sreeramulu S, Jonker HRA, Richter C, Abele R, et al. Structural characterization of the intrinsically disordered domain of Mycobacterium tuberculosis protein tyrosine kinase A. *FEBS Lett*. 2018;**592**:1233–45. <https://doi.org/10.1002/1873-3468.13022>
- 24 Madhurantakam C, Chavali VRM, Das AK. Analyzing the catalytic mechanism of MPTpA: a low molecular weight protein tyrosine phosphatase from Mycobacterium tuberculosis through site-directed mutagenesis. *Proteins Struct Funct Bioinforma*. 2008;**71**:706–14. <https://doi.org/10.1002/prot.21816>
- 25 Zhou P, Wong D, Li W, Xie J, Av-Gay Y. Phosphorylation of Mycobacterium tuberculosis protein tyrosine kinase A PtkA by Ser/Thr protein kinases. *Biochem Biophys Res Commun*. 2015;**467**:421–6. <https://doi.org/10.1016/j.bbrc.2015.09.124>
- 26 Zhou P, Li W, Wong D, Xie J, Av-Gay Y. Phosphorylation control of protein tyrosine phosphatase A activity in Mycobacterium tuberculosis. *FEBS Lett*. 2015;**589**:326–31. <https://doi.org/10.1016/j.febslet.2014.12.015>
- 27 Zhang ZY, Wang Y, Dixon JE. Dissecting the catalytic mechanism of protein-tyrosine phosphatases. *Proc Natl Acad Sci. U. S. A.* 1994;**91**:1624–7. <https://doi.org/10.1073/pnas.91.5.1624>
- 28 Monteiro HP, Arai RJ, Travassos LR. Protein tyrosine phosphorylation and protein tyrosine nitration in redox signaling. *Antioxid Redox Signal*. 2008;**10**:843–89. <https://doi.org/10.1089/ars.2007.1853>
- 29 Alcock LJ, Perkins MV, Chalker JM. Chemical methods for mapping cysteine oxidation. *Chem Soc Rev*. 2018;**47**:231–68.
- 30 van Montfort RLM, Congreve M, Tisi D, Carr R, Jhoti H. Oxidation state of the active-site cysteine in protein tyrosine phosphatase 1B. *Nature*. 2003;**423**:773–7. <https://doi.org/10.1038/nature01681>
- 31 Schieber M, Chandel NS. ROS function in redox signaling and oxidative stress. *Curr Biol*. 2014;**24**:R453–62. <https://doi.org/10.1016/j.cub.2014.03.034>
- 32 Kehm R, Baldensperger T, Raupbach J, Höhn A. Protein oxidation—formation mechanisms, detection and relevance as biomarkers in human diseases. *Redox Biol*. 2021;**42**:101901. <https://doi.org/10.1016/j.redox.2021.101901>
- 33 Tanner JJ, Parsons ZD, Cummings AH, Zhou H, Gates KS. Redox regulation of protein tyrosine phosphatases: structural and chemical aspects. *Antioxid Redox Signal*. 2011;**15**:77–97. <https://doi.org/10.1089/ars.2010.3611>
- 34 Finkel T. Oxidant signals and oxidative stress. *Curr Opin Cell Biol*. 2003;**15**:247–54. [https://doi.org/10.1016/S0955-0674\(03\)00002-4](https://doi.org/10.1016/S0955-0674(03)00002-4)
- 35 Davies MJ. Protein oxidation and peroxidation. *Biochem J*. 2016;**473**:805–25. <https://doi.org/10.1042/BJ20151227>
- 36 Hoshi T, Heinemann S. Regulation of cell function by methionine oxidation and reduction. *J Physiol*. 2001;**531**(Pt 1):1–11. <https://doi.org/10.1111/j.1469-7793.2001.0001j.x>
- 37 Parsons ZD, Gates KS. Thiol-dependent recovery of catalytic activity from oxidized protein tyrosine phosphatases. *Biochemistry*. 2013;**52**:6412–23. <https://doi.org/10.1021/bi400451m>
- 38 Persson C, Sjöblom T, Groen A, Kappert K, Engström U, Hellman U, et al. Preferential oxidation of the second phosphatase domain of receptor-like PTP- α revealed by an antibody against oxidized protein tyrosine phosphatases. *Proc Natl Acad Sci*. 2004;**101**(7):1886–91. <https://doi.org/10.1073/pnas.0304403101>
- 39 Chung HS, Wang S-B, Venkatraman V, Murray CI, Van Eyk JE. Cysteine oxidative posttranslational modifications: emerging regulation in the cardiovascular system. *Circ Res*. 2013;**112**:382–92. <https://doi.org/10.1161/CIRCRESAHA.112.268680>

- 40 Paulsen CE, Carroll KS. Cysteine-mediated redox signaling: chemistry, biology, and tools for discovery. *Chem Rev.* 2013;**113**:4633–79. <https://doi.org/10.1021/cr300163e>
- 41 Jönsson TJ, Murray MS, Johnson LC, Lowther WT. Reduction of cysteine sulfinic acid in peroxiredoxin by sulfiredoxin proceeds directly through a sulfinic phosphoryl ester intermediate. *J Biol Chem.* 2008;**283**:23846–51. <https://doi.org/10.1074/jbc.M803244200>
- 42 Biteau B, Labarre J, Toledano MB. ATP-dependent reduction of cysteine-sulphinic acid by *S. cerevisiae* sulphiredoxin. *Nature.* 2003;**425**:980–4. <https://doi.org/10.1038/nature02075>
- 43 Woo HA, Jeong W, Chang T-S, Park KJ, Park SJ, Yang JS, et al. Reduction of cysteine sulfinic acid by sulfiredoxin is specific to 2-cys peroxiredoxins. *J Biol Chem.* 2005;**280**:3125–8. <https://doi.org/10.1074/jbc.C400496200>
- 44 Bertoldo JB, Rodrigues T, Dunsmore L, Aprile FA, Marques MC, Rosado LA, et al. A water-bridged cysteine-cysteine redox regulation mechanism in bacterial protein tyrosine phosphatases. *Chem.* 2017;**3**:665–77. <https://doi.org/10.1016/j.chempr.2017.07.009>
- 45 Matiello C, Ecco G, Menegatti ACO, Razzera G, Vernal J, Terenzi H. S-nitrosylation of Mycobacterium tuberculosis tyrosine phosphatase A (PtpA) induces its structural instability. *Biochim Biophys Acta.* 2013;**1834**:191–6. <https://doi.org/10.1016/j.bbapap.2012.10.007>
- 46 Zhou H, Singh H, Parsons ZD, Lewis SM, Bhattacharya S, Seiner DR, et al. The biological buffer bicarbonate/CO₂ potentiates H₂O₂-mediated inactivation of protein tyrosine phosphatases. *J Am Chem Soc.* 2011;**133**:15803–5. <https://doi.org/10.1021/ja2077137>
- 47 Dupré-Crochet S, Erard M, Nüße O. ROS production in phagocytes: why, when, and where? *J Leukoc Biol.* 2013;**94**:657–70. <https://doi.org/10.1189/jlb.1012544>
- 48 Stadtman ER, Levine RL. Free radical-mediated oxidation of free amino acids and amino acid residues in proteins. *Amino Acids.* 2003;**25**:207–18. <https://doi.org/10.1007/s00726-003-0011-2>
- 49 Davies MJ, Truscott RJW. Photo-oxidation of proteins and its role in cataractogenesis. *J Photochem Photobiol B Biol.* 2001;**63**:114–25. [https://doi.org/10.1016/S1011-1344\(01\)00208-1](https://doi.org/10.1016/S1011-1344(01)00208-1)
- 50 Grassi L, Cabrele C. Susceptibility of protein therapeutics to spontaneous chemical modifications by oxidation, cyclization, and elimination reactions. *Amino Acids.* 2019;**51**:1409–31. <https://doi.org/10.1007/s00726-019-02787-2>
- 51 Baxter NJ, Williamson MP. Temperature dependence of ¹H chemical shifts in proteins. *J Biomol NMR.* 1997;**9**:359–69. <https://doi.org/10.1023/a:1018334207887>
- 52 Crane EJ, Vervoort J, Claiborne A. ¹³C NMR analysis of the cysteine-sulfinic acid redox center of enterococcal NADH peroxidase. *Biochemistry.* 1997;**36**:8611–8. <https://doi.org/10.1021/bi9707990>
- 53 Mijakovic I, Grangeasse C, Turgay K. Exploring the diversity of protein modifications: special bacterial phosphorylation systems. *FEMS Microbiol Rev.* 2016;**40**:398–417. <https://doi.org/10.1093/femsre/fuw003>
- 54 Hunter T. The genesis of tyrosine phosphorylation. *Cold Spring Harb Perspect Biol.* 2014;**6**:a020644. <https://doi.org/10.1101/cshperspect.a020644>
- 55 Tonks NK. Redox redux: revisiting PTPs and the control of cell signaling. *Cell.* 2005;**121**:667–70. <https://doi.org/10.1016/j.cell.2005.05.016>
- 56 Ehrt S, Schnappinger D. Mycobacterial survival strategies in the phagosome: defense against host stresses. *Cell Microbiol.* 2009;**11**:1170–8. <https://doi.org/10.1111/j.1462-5822.2009.01335.x>
- 57 Klomsiri C, Karplus PA, Poole LB. Cysteine-based redox switches in enzymes. *Antioxid Redox Signal.* 2011;**14**:1065–77. <https://doi.org/10.1089/ars.2010.3376>

Supporting information

Additional supporting information may be found online in the Supporting Information section at the end of the article.

Fig. S1. Oxidative inactivation and reactivation of MptpA.

Fig. S2. NMR spectra of MptpA at nonreducing conditions.

Fig. S3. Oxidative modification of MptpA studied by NMR spectroscopy.

Fig. S4. Backbone dynamics of MptpA.

Table S1. Buffer used for purification of MptpA.

Appendix S1. Materials and methods.